IJCRT.ORG ISSN : 2320-2882

INTERNATIONAL JOURNAL OF CREATIVE RESEARCH THOUGHTS (IJCRT)

An International Open Access, Peer-reviewed, Refereed Journal

Active and Reactive Power Control of DFIG Using a Sliding-Mode and DPC for a Wind Turbines

Abdelkader BOUYEKNI*, Housseyn KAHAL, Rachid TALEB, Zinelaabidine BOUDJEMA

Electrical Engineering Department, Hassiba Benbouali University, Chlef, Algeria
Laboratoire Génie Electrique et Energies Renouvelables (LGEER)

Abstract: The aim of this work is presents a direct power control (DPC) scheme for regulating stator active and reactive power for grid-connected Doubly-Fed Induction Generator (DFIG) .the machine is connected to a public network and operates as a generator. Its rotor is powered by a voltage of two-level inverter. We offer the control of the DFIG by two strategies the first is based on the use of conventional direct power control (C-DPC) with hysteresis regulators and sliding mode control (SMC). Simulation results of proposed controller show successfully effectiveness such as the error between reference and actual values is enforced to zero comparatively to the C-DPC one. Besides, the robustness of machine parameter variation on system conversion simultaneous of wind speed is investigated.

***Keywords*-Wind energy; doubly fed induction generator (DFIG); direct power control; sliding mode control.**

I. INTRODUCTION

Wind energy is the source of the renewable energy that has seen the largest growing rate in the world in the last two decades, mainly because it is considered to be a green energy and economically viable. Variable speed operation of wind turbine is usually used to provide energy with best efficiency. Wind Energy Conversion System (WECS) based on DFIG has several advantages. It reduces stresses of the mechanical structure, acoustic noise reduction and the possibility to regulate both active and reactive power. Another advantage of the DFIG system is that the back-to-back PWM converters, connected between the grid and the induction machine rotor circuit, are sized only for a part of the full power of the generator (about 30%) [1] [2].

Currently, Vector Control (VC) based on Field/Voltage orientation is usually adopted in the control of DFIG-based wind power system, which has a relatively high accuracy. Nevertheless, its closed loop structure with multiple PI regulators reveals several shortcomings such as complex calculation and low dynamic response, which are especially obvious under asymmetrical fault of the grid. DPC uses the rotor-side voltage control to adjust the size and position of rotor flux linkage and regulate the output instantaneous active and reactive power of stator.

Similar to the DTC of asynchronous motor, DPC is a scalar control in itself, the control command of which is much simpler and more direct, easier to realize, and faster because of its few control loop[1-3] [4].

This paper presents a complete modeling and performance comparison for the control of the DFIG WECS connected to the network conventional DPC and SMC-DPC controllers are used. A controller based on SM method is investigated. This type of controllers has proven to be an intriguing method for designing controllers and has been applied in many fields due to its excellent properties, such as insensitivity to some external disturbance and parameters variation [5].

II. MODEL OF DFIG

The schematic diagram of a DFIG-based wind energy generation system is shown in Figure 1 [6].
The model consists of a wind turbine, gearbox and a DFIG. Self-commutated IGBT-based two bi-directional voltage-source converters sharing a common dc link are connected between rotor and stator windings of a DFIG while the stator winding is directly connected to grid.

The model of the DFIG is mainly presented in the literature [7] [8]. In Park reference frame, stator and rotor voltages equations of the generator are given as follows:

$$\begin{cases} V_{ds} = R_s I_{ds} + \frac{d}{dt}\Psi_{ds} - w_s \Psi_{qs} \\ V_{qs} = R_s I_{qs} + \frac{d}{dt}\Psi_{qs} - w_s \Psi_{ds} \\ V_{dr} = R_r I_{dr} + \frac{d}{dt}\Psi_{dr} - w_r \Psi_{qr} \\ V_{qr} = R_r I_{qr} + \frac{d}{dt}\Psi_{qr} - w_r \Psi_{dr} \end{cases} \quad (2.1)$$

where

- V_{ds}, V_{qs},I_{ds} ,I_{qs}, Ψ_{ds} and $\Psi_{qs}$are the voltages, the currents and the fluxes in the two-phase stator circuit.
- V_{dr}, V_{qr},I_{dr} ,I_{qr}, Ψ_{dr} and Ψ_{qr} are the voltages, the currents and the fluxes in the two-phase rotor circuit.

The fluxes of stator and rotor are given by.

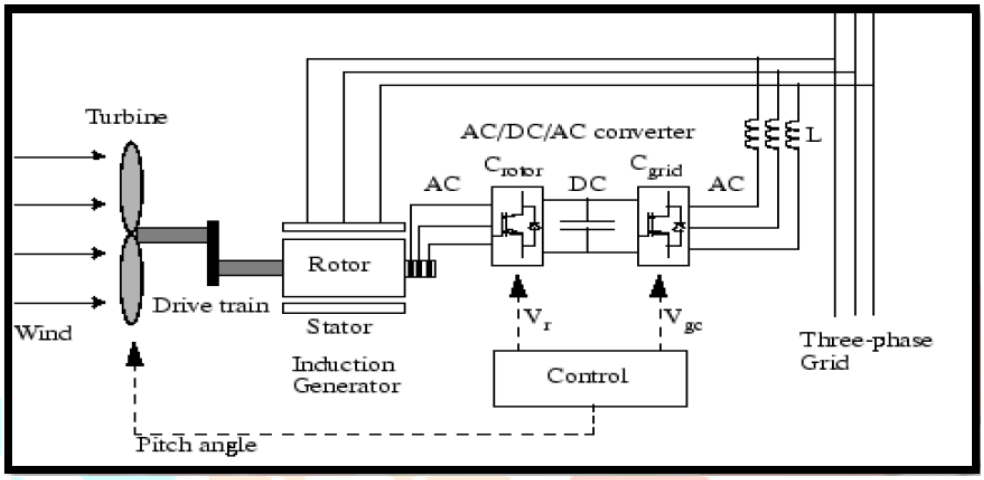

Fig. 1 Configuration of wind system conversion based on DFIG.

$$\begin{cases} \Psi_{ds} = L_s I_{ds} + M I_{dr} \\ \Psi_{qs} = L_s I_{qs} + M I_{qr} \\ \Psi_{dr} = L_r I_{dr} + M I_{ds} \\ \Psi_{qs} = L_r I_{qr} + M I_{qs} \end{cases} \quad (2.2)$$

where the L_s, L_r and M are respectively, the stator, rotor and mutual inductances. Then $L_s = L_{ls} + M$ and $L_r = L_{lr} + M$, L_{ls} and L_{lr} are the leakage inductances stator and rotor; w_s, w_r are the electrical stator and rotor angular speed, linked as following $w_{sl} = w_s - w_r$, is the slip angular speed of the DFIG.

The electromagnetic torque related of mechanical equation of DFIG defined as follow:

$$T_{em} = C_r + J.\frac{d\Omega}{dt} + f.\Omega \quad (2.3)$$

Cr is the load torque, Ω is the mechanical rotor speed, J is the inertia, f is the viscous friction coefficient and p is the number of pole pairs.
where the electromagnetic torque Cem can be expressed as:

$$T_{em} = \frac{3}{2} p \frac{M}{L_s} (\Psi_{qs} I_{dr} - \Psi_{ds} I_{qr}) \quad (2.4)$$

According to the active and reactive powers theory, which is useful for control of power DFIG systems, power stator side components P_s, Q_s can be estimated as:

$$\begin{cases} P_s = \frac{3}{2}(V_{ds} I_{ds} + V_{qs} I_{qs}) \\ Q_s = \frac{3}{2}(V_{qs} I_{ds} - V_{ds} I_{qs}) \end{cases} \quad (2.5)$$

In this part, we use synchronous reference frame of the stator active and reactive power by following state formula when axis d is aligning with the stator flux vector Figure 2.

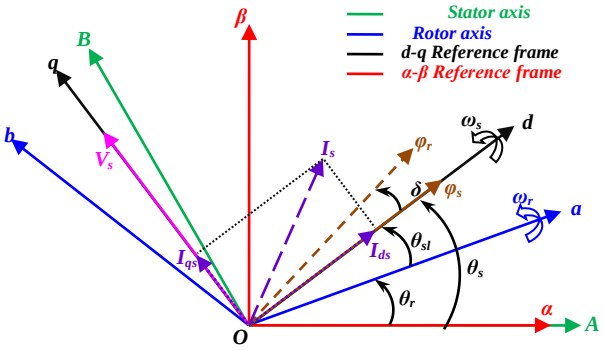

Fig. 2 Field oriented control technique.

by considering the stator resistance *Rs* is ignoring, hence, we can write.

$$\Psi_{ds} = \Psi_s \text{and } \Psi_{qs} = 0 \tag{2.6}$$

$$\begin{cases} V_{ds} = 0 \\ V_{qs} = \omega_s \Psi_s \end{cases} \tag{2.7}$$

$$\begin{cases} I_{ds} = -\frac{M}{L_s} I_{dr} + \frac{\Psi_s}{L_s} \\ I_{qs} = -\frac{M}{L_s} I_{qr} \end{cases} \tag{2.8}$$

Based on (2.6), (2.7), and (2.8), the instantaneous powers of stator can be given as:

$$\begin{cases} P_s = -\frac{3}{2}\frac{\omega_s \Psi_s M}{L_s} I_{qr} \\ Q_s = -\left(\frac{\omega_s \Psi_s M}{L_s} I_{dr} - \frac{\omega_s \Psi_s^2}{L_s}\right) \end{cases} \tag{2.9}$$

The electromagnetic torque can then be expressed by:

$$T_{em} = -\frac{3}{2} p \frac{M}{L_s} I_{qr} \Psi_{ds} \tag{2.10}$$

III. CONTROL OF ACTIVE AND REACTIVE POWER OF DFIG

Figure 3 represents the active and reactive power direct control loop scheme of DFIG:

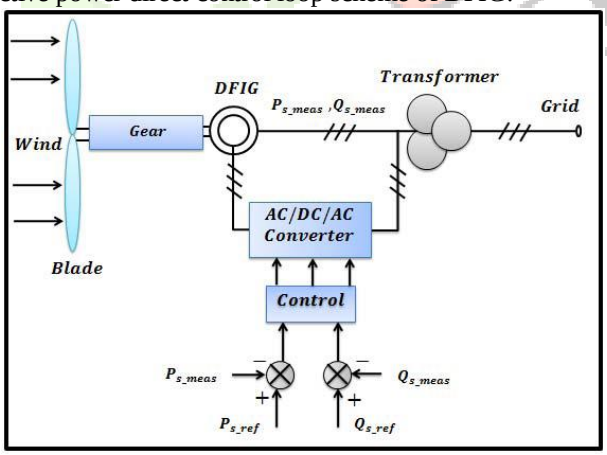

Fig. 3 DFIG Control power between the stator and the grid

To achieve the vector control of stator's active and reactive power as shown on figure 4, a d – q reference frame synchronized with the stator flux was chosen [9] [10]. Stator flux vector is aligned with d-axis, so $\varphi_{ds} = \varphi_s \text{and } \varphi_{ds} = 0$ and the equation of electromagnetic torque becomes:

$$T_e = -\frac{3}{2} P \frac{l_m}{l_s} (\Psi_{ds} I_{dr}) \tag{3.1}$$

The electromagnetic torque and then the active power will only depend on the q-axis rotor current. This torque represents a disturbance for the wind turbine and takes a negative value.

Neglecting the per phase stator resistance R_s(that's the case for medium and high power machines used in wind energy conversion systems) [11], the stator voltages and fluxes can be rewritten as follows:

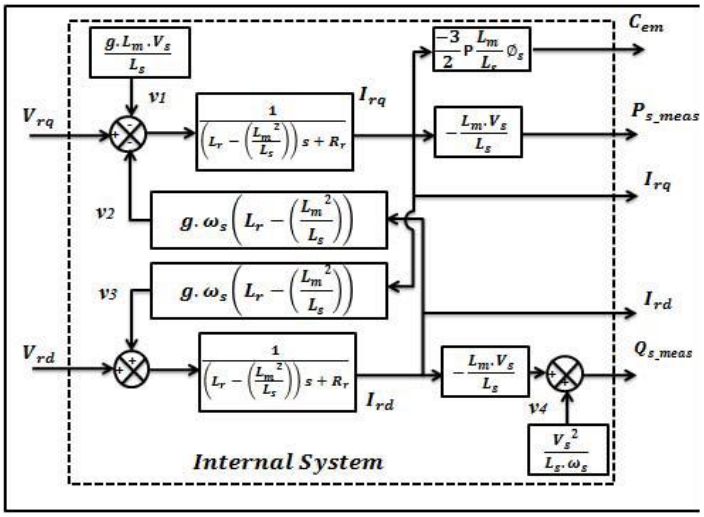

Fig. 4 System power block diagram

3.1 Stator active and reactive power estimation

Instead of measuring the tow powers on the line, we capture the rotor currents, and estimate *Ps* and *Qs*.
This approach gives an anticipated control of the powers in the stator windings. We can find the relations of *Ps* and *Qs* according to both components of the rotor flux in the stationary *αr-βr* reference frame, and we can get:

$$\begin{cases} P_s = -\frac{3}{2}\frac{L_m}{\sigma L_s L_r} V_s \Psi_{\beta r} \\ Q_s = \frac{3}{2} V_s \left(\frac{1}{\sigma L_s}\Psi_s - \frac{L_m}{\sigma L_s L_r}\Psi_{\alpha r}\right) \end{cases} \quad (3.2)$$

Where

$$\begin{cases} \Psi_{\alpha r} = \left(L_r - \frac{L_m^2}{L_s}\right) I_{\alpha r} + \frac{L_m}{L_s}\Psi_s \\ \Psi_{\beta r} = \left(L_r - \frac{L_m^2}{L_s}\right) I_{\beta r} \\ |\overline{\Psi_s}| = \frac{|\overline{V_s}|}{\omega_s} \end{cases} \quad (3.3)$$

If we introducing the flux power angle δ between stator and rotor flux space vectors, P_s and Q_s become:

$$\begin{cases} P_s = -\frac{3}{2}\frac{L_m}{\sigma L_s L_r}\omega_s |\Psi_s||\Psi_r| sin\delta \\ Q_s = \frac{3}{2}\frac{\omega_s}{\sigma L_s}|\Psi_s|\left(\frac{L_m}{L_s}|\Psi_r| cos\delta - |\Psi_s|\right) \end{cases} \quad (3.4)$$

Differentiating (3.4) results in the following equations:

$$\begin{cases} \frac{dP_s}{dt} = -\frac{3}{2}\frac{L_m\omega_s}{\sigma L_s L_r}|\Psi_s|\frac{d(|\Psi_r| sin\delta)}{dt} \\ \frac{dQ_s}{dt} = \frac{3}{2}\frac{L_m\omega_s}{\sigma L_s L_r}|\Psi_s|\frac{d(|\Psi_r| cos\delta)}{dt} \end{cases} \quad (3.5)$$

Note that δ is the included angle of stator and rotor magnetic linkage in the rotor orientation coordinate system.
From (3.5), the plus-minus of $d(|\Psi_r|sin\delta)$ and $d(|\Psi_r|cos\delta)$ will directly influence the plus-minus of the change rate of the active and reactive power, i.e., the variation tendency of power is influenced, which illustrates that the control of stator's power (Ps, Qs) can transform to the control of rotor's magnetic linkage (Ψ_r). Omitting rotor's resistance, the differential of rotor's magnetic linkage is expressed as:

$$\frac{d\Psi_r}{dt} = V_r - R_r I_r \approx V_r \quad (3.6)$$

According to (3.6), the differential of rotor flux is due to the changes of rotor voltage: Ψ_r moves in the direction of V_r, with the speed proportionally to $|V_r|$. Then the motion of rotor flux vector will be controlled based on the proper selection of switching vector. Accordingly, set switching table and it makes up the conventional DPC. DPC based on hysteresis Control and look-up table method is Band-Band control essentially, whose switching frequency variation complicates the power circuit and filter design. Apply space vector pulse width modulation (SVM) to achieve fixed switching frequency [12] [13], and calculate the voltage vector

that should output in one sampling period according to the relationship of instantaneous power and reference values, is the DPC in this paper.

3.2 Principle of SVM

SVM separates the space into six sectors (*Sn*, n=1-6), based on the eight basic space vectors (non zero vector *V1-V6*, zero vector *V0* & *V7*) composed by the eight combinations of the 3-phase convertor's switching states, as Figure 5 shows. According to the *Sn* of reference space vector *Vr*, two adjacent effective vectors (*Va, Vb*) and zero vector (*Vzero*) are selected to operate. Calculate the acting time of every vector (*Ta, Tb & Tzero*), and distribute *Tzero* symmetrically through the sampling period (*TSVM*). Finally the switching signals of the convertor (*Sa, Sb, Sc*) are determined.

In each *TSVM*, this calculation operates and convertor's switching state change for once. The higher the modulation frequency is, the better the operation effects will be, while the request to the switching tubes will also be stricter. SVM model is achieved based on MATLAB/Simulink, and applied in the DPC model in this paper.

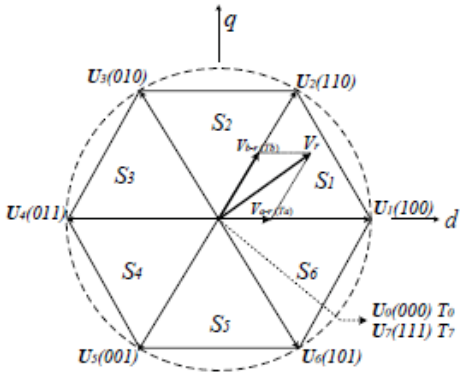

Fig. 5 Graph of basic voltage space vector

IV. Sliding Mode Controller Design

The SMC controller has been very successful in recent years. This is due to the simplicity of its implementation and its robustness against the uncertainties of the system and external disturbances in the process. Sliding mode control is to bring back the state trajectory to the sliding surface and to advance on it with a certain dynamic point balance (Figure 6) [12] [13]. This trajectory determination consists of three parts.

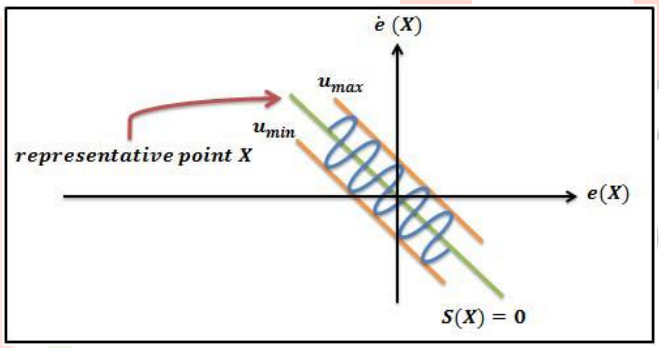

Fig. 6 Trajectory mode in the phase plane

4.1 Choice of the sliding surface

For a nonlinear system presented in the following form:

$$\begin{cases} \dot{X} = f(X,t) + g(X,t) \\ X \in \Re^n, u \in \Re \end{cases} \quad (4.1)$$

Where $f(X,t)$ and $g(X,t)$ are two non-linear continuous functions and uncertain assumed bounded. It takes the form of the general equation proposed by J. J. Slotine to determine the slip surface [12] [13]:

$$\begin{cases} S(X) = \left(\frac{d}{dt} + \lambda\right)^{n-1} e \\ e = X^d - X \end{cases} \quad (4.2)$$

Where e is the size to resolve error, λ is a positive coefficient, n is relative degree, X^d is the desired greatness:
$X^d = [x^d, \dot{x}^d, \ddot{x}^d, \dots]^T$, X^d is the state of the ordered size variable:
$X = [x, \dot{x}, \dots, x^{n-1}]^T$

4.2 The convergence condition

The convergence condition is defined by the equation of Lyapunov [12] [13]. It makes the surface attractive and invariant:

$$(S(X))\left(\dot{S}(X)\right) \leq 0 \qquad (4.3)$$

4.3 Computation of the control

The control algorithm is defined by the relationship:

$$u = u^{eq} + u^{n} \qquad (4.5)$$

where: is the size of control signal, u^{eq}: size of equivalent control signal, u^{n}: switching control term.

$$u^{n} = u^{max} sat(S(X)/\emptyset) \qquad (4.6)$$

$$sat(S(X)/\emptyset) = \begin{cases} sig(s) & si|s| > \emptyset \\ s/\emptyset & si\ |s| < \emptyset \end{cases} \qquad (4.7)$$

$sat(S(X)/\emptyset)$: Saturation function, $\emptyset$: width of the threshold saturation function.
The simplest solution satisfying this condition (equation 19) has the form

$$\begin{cases} u^{n} = cKsign(S(X)) \\ K > 0 \end{cases} \qquad (4.8)$$

Active and reactive powers can be expressed as the derivative of sliding surface

$$\begin{cases} \dot{S}(P) = \left(\dot{P}_{s-ref} - \dot{P}_{s-mes}\right) \\ \dot{S}(Q) = \left(\dot{Q}_{s-ref} - \dot{Q}_{s-mes}\right) \end{cases} \qquad (4.9)$$

From equation 1.2, the derivative expressions of active and reactive power are:

$$\begin{cases} \dot{S}(P) = \left(\dot{P}_{s-ref} - V_s \frac{L_m}{L_s} \dot{I}_{rq}\right) \\ \dot{S}(Q) = \left(\dot{Q}_{s-ref} - V_s \frac{L_m}{L_s} \dot{I}_{rd}\right) \end{cases} \qquad (4.10)$$

$$\begin{cases} \dot{S}(P) = \left(\dot{P}_{s-ref} - V_s \frac{L_m}{L_s L_r \sigma} (V_{qr} - R_r I_{qr})\right) \\ \dot{S}(Q) = \left(\dot{Q}_{s-ref} - V_s \frac{L_m}{L_s L_r \sigma} (V_{dr} - R_r I_{dr})\right) \end{cases} \qquad (4.11)$$

Replacing V_{rq} by $V_{rq}^{eq} + V_{rq}^{n}$, and V_{dr} by $V_{rd}^{eq} + V_{rd}^{n}$

$$\begin{cases} \dot{S}(P) = \left(\dot{P}_{s-ref} - V_s \frac{L_m}{L_s L_r \sigma} (V_{rq}^{eq} + V_{rq}^{n} - R_r I_{qr})\right) \\ \dot{S}(Q) = \left(\dot{Q}_{s-ref} - V_s \frac{L_m}{L_s L_r \sigma} (V_{rd}^{eq} + V_{rd}^{n} - R_r I_{dr})\right) \end{cases} \qquad (4.12)$$

Which was derived previously, and then the greatness of the equivalent command V_{qr}^{eq} and V_{dr}^{eq} can be written as:

$$\begin{cases} V_{qr}^{eq} = \left(-\dot{P}_{s-ref} \frac{L_s L_r \sigma}{L_m V_s} + R_r I_{qr}\right) \\ V_{dr}^{eq} = \left(-\dot{Q}_{s-ref} \frac{L_s L_r \sigma}{L_m V_s} + R_r I_{dr}\right) \end{cases} \qquad (4.13)$$

During the sliding mode and steady state, we have:

$$\begin{cases} S(P) = 0\ and\ S(Q) = 0 \\ \dot{S}(P) = 0\ and\ \dot{S}(Q) = 0 \\ V_{rq}^{n} = 0\ and\ \ V_{rd}^{n} = 0 \end{cases} \qquad (4.14)$$

During the convergence mode, the condition for $S(P)\dot{S}(P) \leq 0$ and $S(Q)\dot{S}(Q) \leq 0$ is verified, we set:

$$\begin{cases} \dot{S}(P) = \left(-V_s \frac{L_m}{L_s L_r \sigma} V_{rq}^{n}\right) \\ \dot{S}(Q) = \left(-V_s \frac{L_m}{L_s L_r \sigma} V_{rd}^{n}\right) \end{cases} \qquad (4.15)$$

$$\begin{cases} V_{rq}^{n} = K_1 sign(S(P)) \\ V_{rd}^{n} = K_2 sign(S(Q)) \end{cases} \quad (4.16)$$

V. SIMULATION RESULTS AND DISCUSSIONS

In this part simulations are carried out with a 1.5 MW DFIG attached to a 398 V/50 Hz grid, by using the environment of Matlab/Simulink. Parameters of the machine are given in the Table 5.1. The both control strategies C-DPC, and SMC-DPC are simulated and compared regarding reference tracking, stator current harmonics distortion, responsiveness to the rotor speed variation and robustness against machine parameter variations.

TABLE 5.1 THE DFIG PARAMETERS.

Parameters	Rated Value	Unity
Nominal power	1.5	MW
Stator voltage	398	V
Stator frequency	50	Hz
Number of pairs poles	2	
Stator resistance	0.012	Ω
Rotor resistance	0.021	Ω
Stator inductance	0.0137	H
Rotor inductance	0.0136	H
Mutual inductance	0.0135	H
Inertia	1000	Kg m2
Viscous friction	0.0024	Nm/s

5.1 Reference tracking

The main of this test is to verify the performance of proposed strategy when the DFIG's speed is considered constant at its nominal value. The obtained simulated results are shown in Figures 7-9. As it's presented by Figures 7 and 8, both controllers, the active and reactive power tracks correctly their references steps and there is no Static error. Furthermore, it can be observe that the SMC-DPC ensures the decoupling between the two axes contrary to the C-DPC. Further tests were carried out, in Figure 9, it can be seen the total harmonic distortions (THD) of stator current of the generator by using Fast Fourier Transform (FFT) method for both DPC control schemes. It is clearly seen that the SCM-DPC control reduces the (THD) (THD = 0.59 %) compared with C-DPC (THD = 4.95%), because it alleviates the phenomenon of chattering.

5.2 Robustness test

The robustness of the proposed DPC based SMC algorithm during the machine running at its nominal speed is analyzed for the changing machine's parameters. Such as the variations in the values of the stator and rotor resistances and the values of inductances has to be taken into account for checked robustness of the regulation scheme in the simulation. For this reason the values of the resistances R_s and R_r doubled and the values of the inductances L_s, L_r and M are divided by 2. Simulation results are shown in Figures 10-12 as it's seen by these figures, it can be clearly observed that hardly any differences with such large parameter variations values of the DFIG for proposed SMC-DPC scheme contrary to the C-DPC strategy where the time response is increase slightly. Therefore, robustness of the novel SMC-DPC scheme to DFIG parameters' variations is also approved.

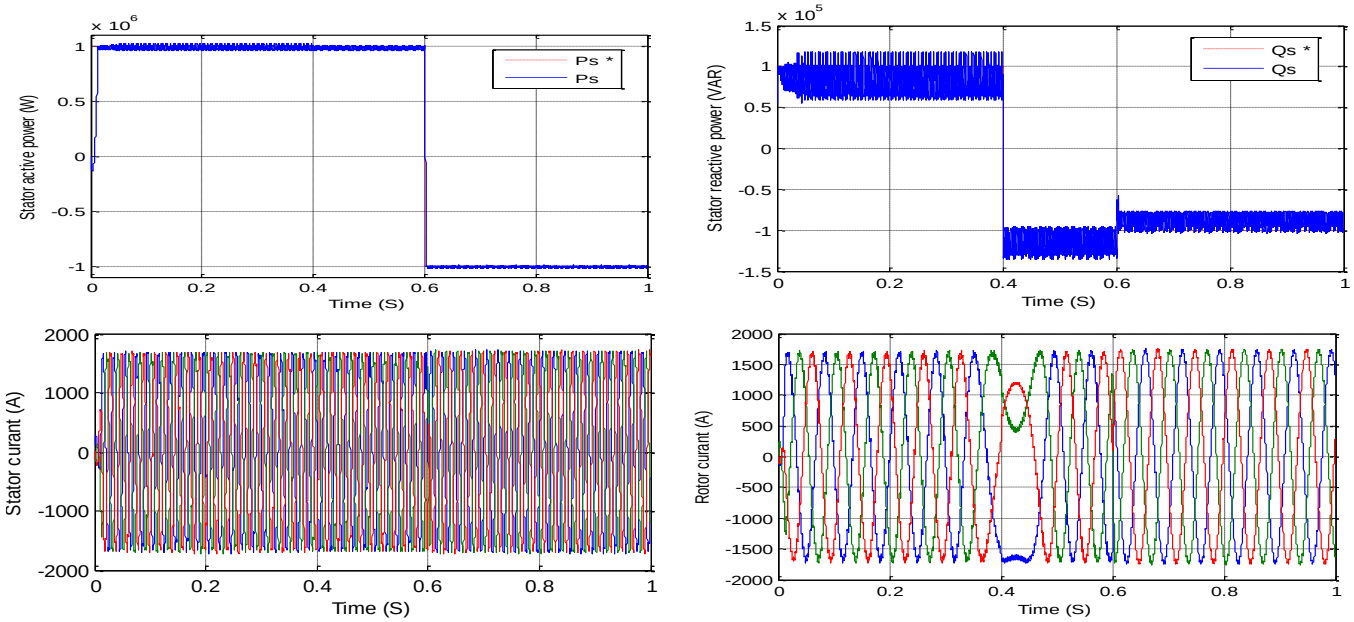

Fig. 7 C-DPC strategy responses (reference tracking test).

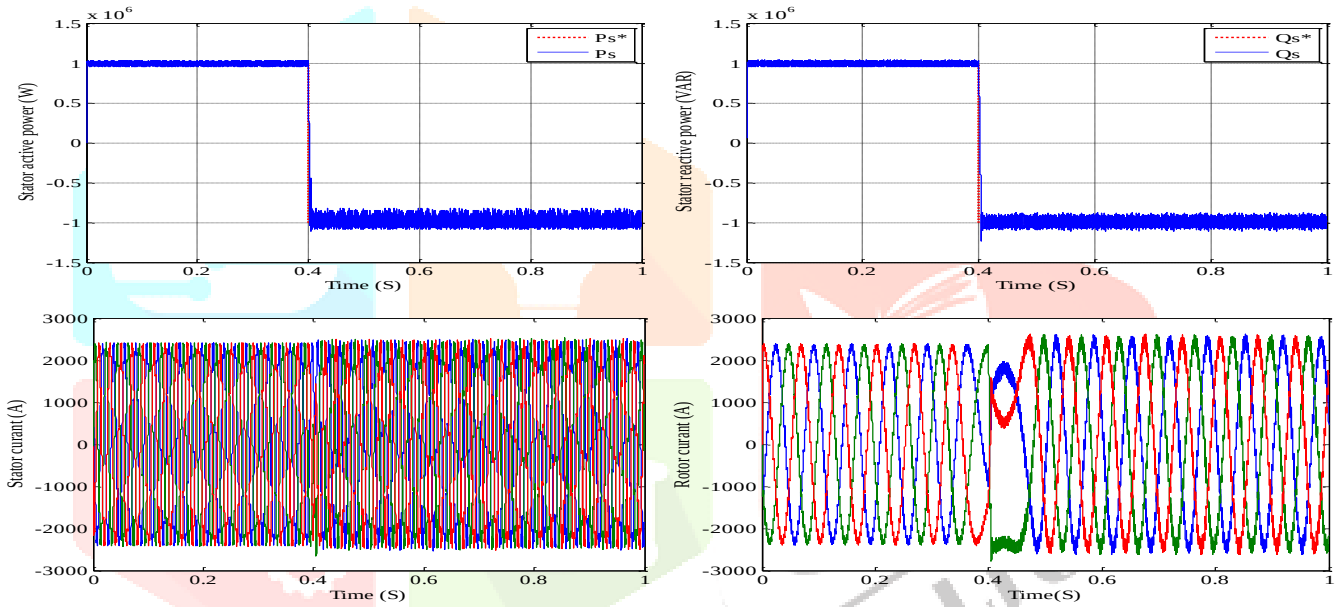

Fig. 8 SMC-DPC strategy responses (reference tracking test).

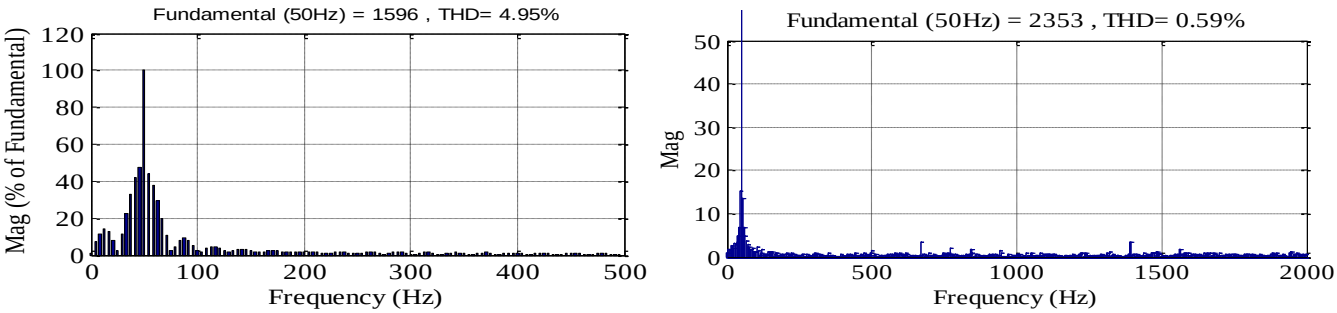

(a) : C-DPC (b) : SMC-DPC

Fig. 9 Spectrum harmonic of one phase rotor current.

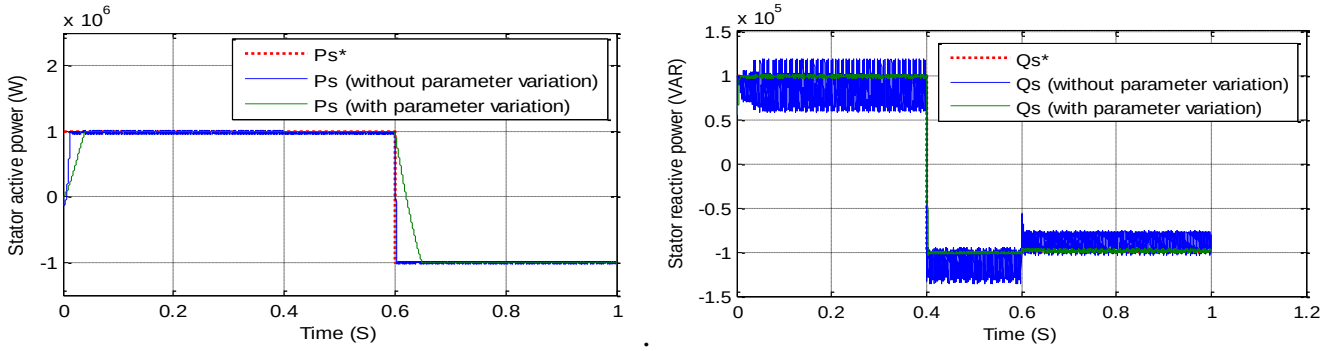

Fig. 10 C-DPC strategy responses (robustness test).

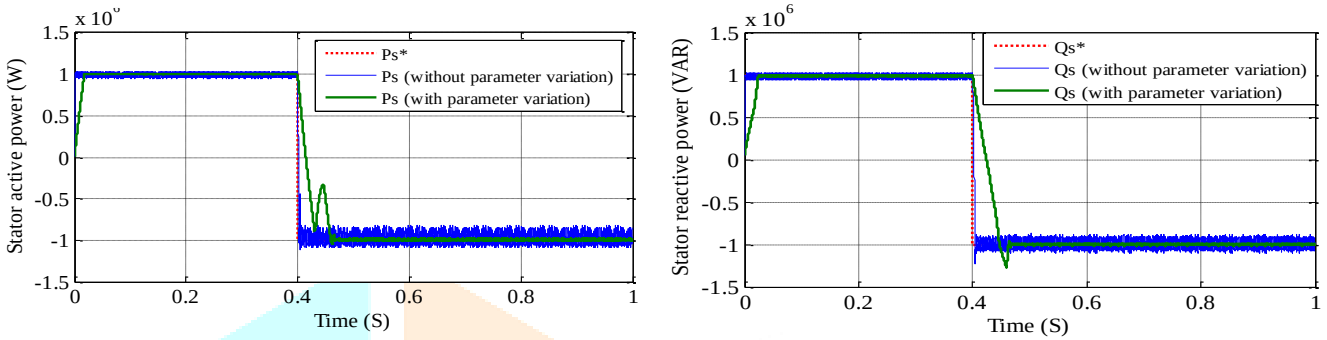

Fig. 11 SMC-DPC strategy responses (robustness test).

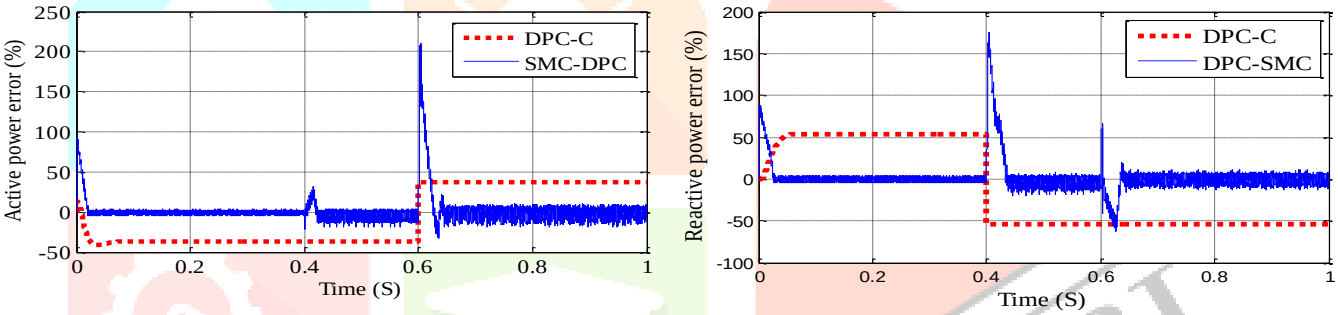

Fig. 12 Error curves (robustness test).

VI. CONCLUSION

A SMC-DPC strategy for DFIG using active and reactive power has been proposed in this paper. The proposed DPC has been implemented on 1, 5 MW wind turbine-DFIG system. The results indicate that the proposed SMC-DPC preserves the main properties of conventional DPC mode, has good robustness to parameters variations. The simulation results verify also that the proposed control strategy has not only good steady state performance but also good dynamic performance.

VII. REFERENCES

[1] Jay, D and Mihir R. 2018. Modeling and simulation of DFIG based wind-farm for constant power control and fault-ride through. IJCRT, 6(1): 2320-2882

[2] Ahmed T, Nishida K and Nakaoka M. 2007 A novel stand-alone induction generator system for AC and DC power applications. IEEE 43: 1465-1474.

[3] Zhang J. F, Mao Ch. X, Lu J. M and Wu J. D. 2006. Direct power control strategy of doubly fed induction generator. Electric Power Automation Equipment, vol 24, No 6, pp. 31-35

[4] Hamane B, Doumbia M. L, Bouhamida A. M and Benghanem M. 2014. Direct active and reactive power control of DFIG based WECS using PI and sliding mode controllers. IEEE Industrial Electronics Society, pp. 2050-2055.

[5] Hu J, Nian H, Hu B, He Y and Zhu Z. 2010. Direct active and reactive power regulation of DFTG using sliding-mode control approach. IEEE Trans. Energy Convers., vol. 25, no. 4, pp. 1028-1039.

[6] Li S and Haskew T. 2009. Energy Capture, Conversion, and Control Study of DFIG Wind Turbine under Weibull Wind Distribution. IEEE power and energy society general meeting (PES), pp 1-9.

[7] Kahla S, Soufi Y, Sedraoui M and Bechouat M. 2015. On-Off control based particle swarm optimization for maximum power point tracking of wind turbine equipped by DFIG connected to the grid with energy storage. Int J Hydrogen Energ, vol.40, pp.13749-13758.

[8] Bakouri A, Abbou A. Mahmoudi H and Elyaalaoui K. 2014. Direct torque control of a doubly fed induction generator of wind turbine for maximum power extraction. IEEE International Renewable and Sustainable Energy Conference, pp. 334-339.

[9] Poitiers F, Machmoum M, Le Doeuff R and Zaim M.E. 2001. Control of a doubly-fed induction generator for wind energy conversion systems. IEEE Trans. Renewable Energy, Vol. 3, N°. 3 pp.373-378.

[10] Mai T.D, Mai B. L,Pham D.T and Nguyen H.P. 2007. Control of doubly-fed induction generators using Dspace R&D controller board – an application of rapid control coordinated with Matlab/Simulink. International Symposium on Electrical & Electronics Engineering, Track. 3, pp 302-307.

[11] Zhang L, Watthansarn C. and Shehered W. 2002. A matrix convertervexcited doubly-fed induction machine as a wind power generator. IEEE Trans.Power Electronics and Variable Speed Drives, vol. 2, pp 532 – 537.

[12] Dawei Zhi, Lie Xu. Direct Power Control of DFIG With Constant Switching Frequency and Improved Transient Performance. IEEE Trans on Energy conversion, 2007, vol 22, No 1, pp.110-118.

[13] Kim W. S, Jou S. T, and Lee K. B. 2008. Direct Power Control of a Double Fed Induction Generator with a Fixed Switching Frequency. Industry Applications Society Annual Meeting. IAS'08. IEEE, pp.1-9.

[14] Machmoum M, Poitiers F, Darengosse C. and Queric A. 2002. Dynamic Performances of a Doubly-fed Induction Machine for a Variablespeed Wind Energy Generation," IEEE Trans. Power System Technology, vol. 4, pp. 24